IEEE Transactions on Nuclear Science, Vol. NS-30, No. 4, August 1983

THE MONTREAL ELECTRON ACCELERATOR PROPOSAL

G.K. Bavaria, P. Depommier, P. Hinrichsen, H. Jeremie,
Louis Lessard and J.P. Martin

Laboratoire de Physique Nucléaire, Université de Montréal,
Montréal, Canada H3C 3J7

SUMMARY

A 50 MeV CW RTM electron accelerator has been designed at the University of Montreal. The system consists of an electron gun, a chopper-buncher, a preaccelerator and the 50 MeV RTM. The installation is essentially the first phase of what is hoped will one day be a 1 GeV Canadian electron facility. A general outline of the system is presented. The main topics discussed are the various system components, the beam optics calculations and some of the experimental equipment to be used in the proposed nuclear physics research program.

INTRODUCTION

For the last several years nuclear physicists at the University of Montreal have been keenly interested in developing a CW electron facility in the Montreal area. In November of 1981 we submitted a proposal (1) outlining our ideas for a 1 GeV Canadian electron facility consisting of three accelerator stages (20 MeV RTM, 200 MeV RTM and a 1 GeV RTM or DSM). In addition we requested funds for the design and construction of the 3.5 MeV injector and the first stage 20 MeV RTM.

However, NSERC (the Canadian granting agency) as well as many interested Canadian physicists recommended that this low energy machine should be justified on the basis of a viable nuclear physics research program. After carrying out a detailed study of the type of physics research that could be done with low energy electron and photon beams we concluded that the experimental possibilities would indeed be rich if the energy of this first stage was increased to at least the 50 MeV level. This would allow us to carry out significant research programs in electro- and photo-fission, giant multipole resonances, (e,e') and (e,e'x) experiments as well as experiments using polarized photons and others.

In July 1982 we submitted a second proposal (2) to NSERC requesting funds to build the 50 MeV RTM CW electron facility. Our prime interest is still in the 1 GeV facility and we emphasize that we regard this machine as an injector stage of a Canadian electron facility. In effect, our proposal is similar to that of the Mainz group (3) who started with a 14 MeV RTM and who have now essentially completed their second stage 185 MeV RTM.

The RTM Injector

The role of the injector is to provide a tightly bunched beam matched to the acceptance of the RTM and having a sufficiently high energy so as to maintain the phase slip within reasonable limits after each recirculation through the RTM LINAC. A schematic of the injector system is shown in Fig. I. It consists of:

1) A 100 keV electron gun,
2) A chopper-buncher system,
3) A 1.27 MeV graded-β LINAC,
4) Two 1.5 MeV $\beta = 1$ LINACS.

The Electron Gun: The Koontz-Miller gun design developed at SLAC for the NBS-LASL microtron will be used to provide an electron beam with the following characteristics:

Beam energy:	100 keV
Beam current:	0 to 5 mA DC
Beam emittance:	4π mm-mrad
Max. rep. rate:	25 MHz
Min. pulse length:	2.5 ns

A pulsed beam mode of the electron gun is also required for beam diagnostics and tuneup of the system, as well as for the single microcycle mode of operation. Tuneup is carried out by following a single beam pulse through the system and thus pulses shorter than the recirculation time in the RTM ($\sim$12 ns) are required. The repetition rate will be typically of the order of 10 kHz when the beam monitor signal is to be computer processed.

The Chopper-Buncher: The chopper buncher (see Fig.I) is similar in design to the system that has been developed at NBS (4) for the 185 MeV RTM. The initial beam emittance is set by the focusing solenoids, L_1 and L_2, and the two emittance limiting apertures, A_1 and A_2. These elements provide an electron beam with an emittance of 4π mm-mrad. The beam is then deflected off axis by C_1, the first transverse deflecting cavity, which causes the beam to trace out a circle of radius 5 mm on the chopper plate, A_3. A 60° slot

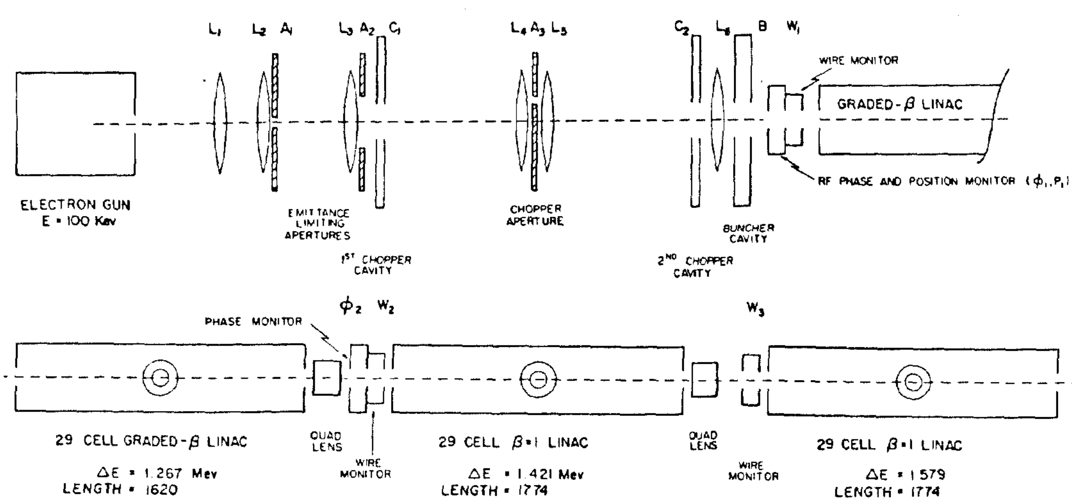

Fig. I: Schematic layout of the RTM injector showing the chopper buncher, graded-β and the $\beta = 1$ LINACS.

(dimensions in mm)

0018-9499/83/0800-3291$01.00© 1983 IEEE

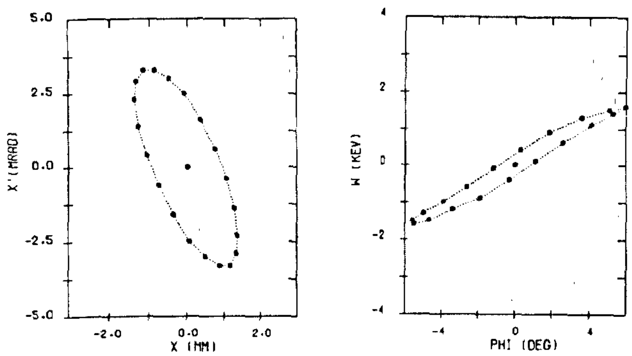

Fig. II: Transverse(A) and Longitudinal (B) phase space of the beam at the entrance of the graded-β LINAC.

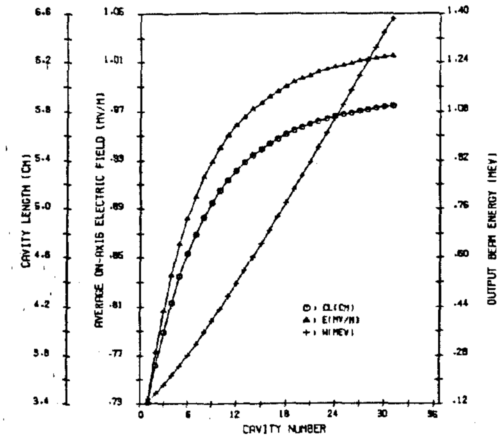

Fig. IV: Plot of cavity length, average axial electric field and beam energy as a function of cavity number for the graded-β LINAC.

cut out of this plate allows 1/6 of the beam to pass through with a relative RF phase of ±30°. The beam is then bent back toward the axis by the split solenoid L_4 and L_5 where it passes through the second deflecting cavity, C_2, which cancels effect of C_1 and produces a beam parallel to the system axis.

The beam then passes through the bunching cell. The amount of bunching required is determined by the acceptance of the graded-β LINAC and is controlled by the RF amplitude in the buncher and the drift space between the buncher and the graded-β LINAC. In the present design the optics have been calculated with PARMELA (5) starting with an initial transverse phase space area of 4π mm-mrad and a longitudinal phase space of 5π keV-deg. The emittance of the beam at the entrance of the graded-β LINAC is shown in Fig. II. PARMELA has also been used to calculate the transmission of the beam through the β = 1 LINACS. For the 29 cell structures being proposed the calculations indicate excellent transmission when focusing quadrupoles are interposed between the LINACS (see Fig. I). The calculations predict the beam emittance at the exit of the second β = 1 LINAC shown in Fig. III.

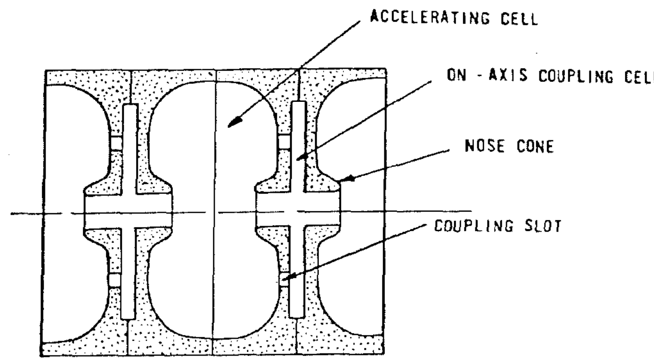

Fig. V: Cut-away view of an on-axis coupled structure.

The LINAC Structures: All of the structures to be used are made up of 29 accelerating cells. For the graded-β LINAC calculations with PARMELA allow one to optimize the maximum electric field permissible with the injection phase so that the best beam transmission is obtained. The results of these calculations are

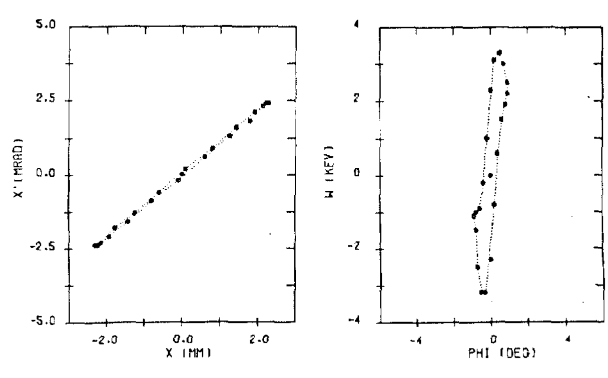

Fig. III: Transverse(A) and Longitudinal(B) phase space of the beam at the exit of the second β = 1 LINAC.

shown in Fig. IV for a synchronous phase of -10°. We have adopted the π/2 biperiodic on axis coupled structure without radial cooling presently in use at Mainz (3) rather than the more complicated radially cooled design of CRNL (6). A cutaway view of this cell design is shown in Fig. V. Coupling slots cut into the flat portion of the web and located as far as possible from the structure axis allow magnetic coupling between the RF modes in the accelerating and coupling cells. From Fig. IV it can be seen that the lengths of the first several cells of the graded-β LINAC are such that the nose to nose separation will be rather small as the length of the coupling cells is independent of the β of the accelerating cells. To overcome this difficulty the first eight cells of this structure will have the nose cones cut back. This would normally result in accelerating cells that are poorly tuned. However, the cells can be brought back into tune by adjusting the radial dimension. The cells will then have a shunt inpedance considerably lower than the optimum value. This, however, causes little difficulty since reserve power is available from the graded-β LINAC klystron. The rest of this accelerating structure as well as the two succeeding β = 1 LINACS will be of the standard cell design optimized for shunt impedance using the SUPERFISH (7) code.

THE RACETRACK MICROTRON

The basic properties of the RTM are its resonance condition and its beam acceptance and emittance. These three properties are interdependent and define the beam energy and emittance requirements of the injection system. The resonance condition requires that the time of flight between successive orbits be an integral multiple of the RF period in the LINAC. For the ideal case of a hard edge magnetic field and purely relativistic particles this condition leads to the following relation between the energy gain per turn, ΔE, and the magnetic field, B:

$$2\pi\ \Delta E/eBC = n\lambda\ .$$

The spacing, d, between successive orbits is given by:

$$d = n\lambda/\pi$$

where n is the number of wavelengths by which the orbit circumference is increased from one turn to the next.

The choice of n thus determines the size of the machine as well as the required field in the end magnets. Finally, the energy gain per circulation through the RTM LINAC is:

$$\Delta E = \sqrt{ZPL}\ \cos\phi$$

where:

- ϕ is the synchronous phase,
- Z is the shunt impedance/unit length,
- P is the power/unit length,
- L is the length of the RTM LINAC.

The resonance condition for particles travelling at a velocity close to that of the speed of light is never quite attained in the RTM and hence there is a phase slip of the beam from turn to turn with respect to the RF field. The RTM, however, exhibits a phase stability similar to that in circular accelerators. Thus if a beam of particles arrives with a phase different from the synchronous phase its phase on successive orbits will oscillate about the synchronous phase.

The selection of the value of n is a choice between a large inter-orbit gap and the need to preserve as much of the longitudinal acceptance as possible. It was felt that a 4 cm ($\sim\lambda/\pi$) orbit spacing was acceptable and so, as at Mainz, we chose n = 1.

To avoid excessive vertical defocusing and to provide adequate clearance of the RTM LINAC on the return path of the first orbit we chose ρ to be 6 cm. For the 4.37 MeV electron beam we have:

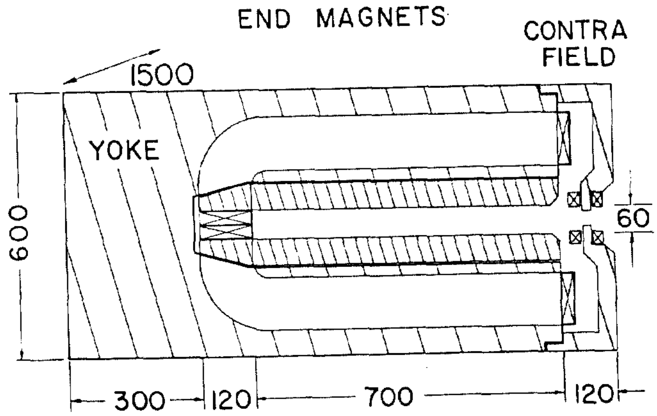

Fig. VII: Schematic of the RTM end magnets showing the contrafield poles (*dimensions in mm*)

$$B\rho = 0.0162\ \text{T-m}\ .$$

Thus, for a first orbit radius of 6 cm the field is:

$$B = 0.272\ \text{T}$$

and from the resonance condition for n = 1 the energy gain per turn is:

$$\Delta E = 1.58\ \text{MeV}\ .$$

The selection of the basic RTM parameters is seen to be in accord with the rule-of-thumb that the optimal one pass energy gain should be approximately 1/3 the injected beam energy. A schematic of the proposed RTM is shown in Fig. VI.

<u>RTM End Magnets</u>: The end magnets provide a highly uniform field over the area of the pole faces adjacent to the recirculating beam. The size of these magnets depends on the diameter of the last orbit, which, for the present design, is 117.6 cm. Thus, the end magnets must have a highly uniform field region extending over an area of at least 60 cm x 120 cm.

The degree of uniformity required is estimated from the longitudinal acceptance of the RTM. An n = 1 RTM is stable against small perturbations if the beam phase at the LINAC falls between the limits (8):

$$0 \le \phi \le \tan^{-1}(2/n\pi) = 32.5^{\circ}.$$

Fig. VI: Schematic layout of the proposed 50 MeV CW RTM. (Dimensions in mm).

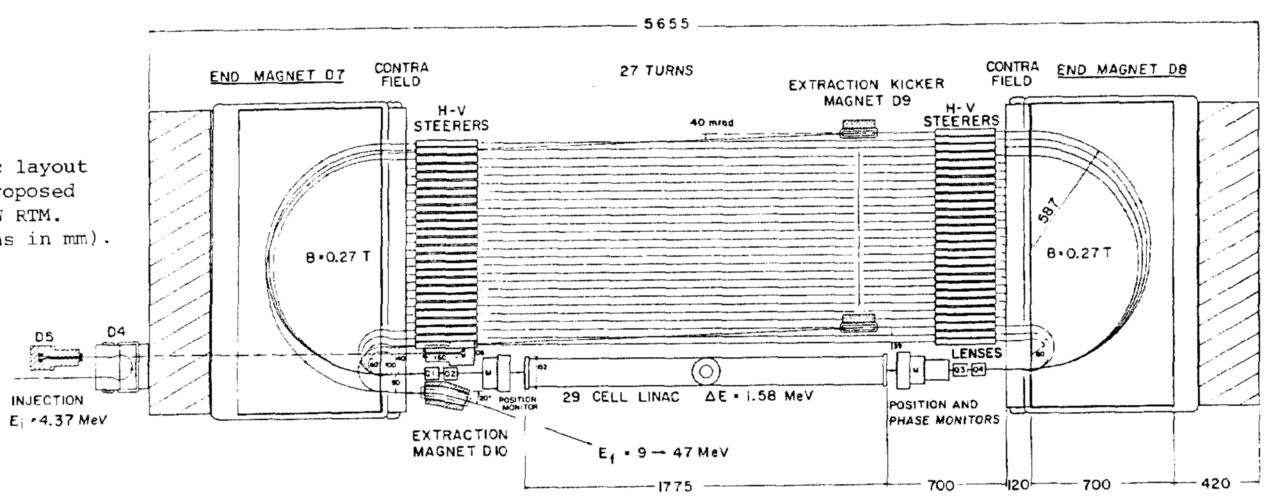

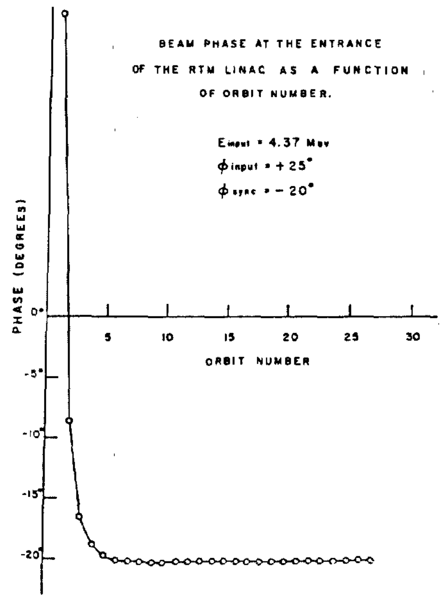

Fig. VIII: Beam phase at the entrance of the RTM LINAC as a function of orbit number.

It is desirable to keep the magnitude of the phase variation due to the field errors to less than 1°. Since the last beam orbit has a total length in the end magnet of 185.2 cm, which is equivalent to 5570 degrees of phase, we see that an integrated error in the field of 2×10^{-4} will introduce a phase error of 1 degree.

Recently, Debenham (9) at NBS has developed a new RTM end magnet design which allows one to obtain such uniformities relatively easily. This half picture frame geometry provides a field that is uniform over a large fraction of the physical gap. The geometry is further improved by incorporating a double gap Purcell filter (see Fig. VII) into this design. By using two different gaps, one in the coil region and the other in the main field region, a field uniformity of 2×10^{-4} can be achieved without difficulty.

The end magnets were designed by using magnetostatic computer codes such as TRIM (10) and PANDIRA (11). To produce the final required field uniformity, a 0.15 cm shim was needed between the yoke and the pole piece extending 25 cm into the magnet. The magnet gap of 6 cm was chosen in order to permit the installation of an independent vacuum box as well as any corrective pole face windings (12) that may be required. These windings are low-powered printed circuit board correction coils and are placed next to the pole faces.

The RTM Linac: In order to minimize costs we have decided to use identical $\beta = 1$ structures throughout the system. Thus, as in the injector, the RTM LINAC is made of 29 accelerating cells all of length 6.118 cm. The field gradient is 0.95 MV/m, a value that has been successfully used at Mainz. The cell design is optimized by SUPERFISH calculations and the results indicate a shunt impedance of 67 MΩ/m.

The fact that the injected beam has a β of 0.995 causes no particular problems. Beam dynamics calculations with PTRACE (13) give among other results the beam phase at the entrance of the LINAC. In Fig. VIII it can be seen that for an injection phase of $+25^{\circ}$ the beam phase at the LINAC entrance on successive orbits rapidly approaches the synchronous phase. In fact, after the sixth orbit, where the beam energy is 13 MeV, no further phase slip occurs and only a slight oscillation ($\pm 0.2^{\circ}$) is present.

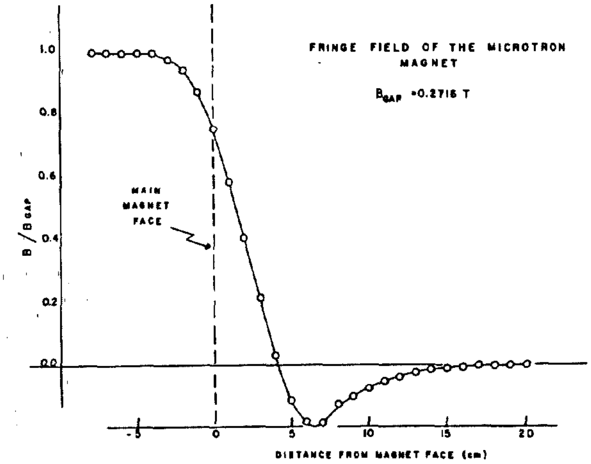

Fig. IX: Fringe field of the RTM magnet.

The RTM Optical System: Several optical designs have been proposed for RTM beam control. The most notable are the Illinois MUSL design (14), the NBS design (4) and the Mainz design (3). We have chosen to adopt the Mainz technique. The advantages of this design are its low cost and simplicity. The system requires only two symmetrical quadrupoles on the LINAC axis which have their strengths adjusted so that the first pass focal length in both transverse planes is approximately equal to 1/3 the distance between the RTM magnets. This provides the required strong focusing in the critical early orbits and does not couple the longitudinal and transverse emittances of the beam. The disadvantage of this system is that as the energy of the beam increases the focal lengths of the quadrupoles grow as the square of the beam energy. This prevents the beam from compressing transversely as the energy grows and makes it more sensitive to magnetic non-uniformities. Eventually these lenses become so weak that a large number of orbits are required to return a displaced beam to the system axis.

Another factor that must be taken into consideration is the effect of the fringe fields of the end magnets. The axial component of the fringing field of a simple pole edge produces a vertical defocusing effect on the beam. This field also deforms the beam trajectories causing phase errors. These difficulties are overcome by introducing the contrafield poles (15) shown in Fig. VII. With this system the axial component of the field exhibits a much steeper fall-off and an undershoot while a wider field free region is obtained (see Fig. IX).

With this optical system the orbits of the beam through 27 turns in the RTM were calculated using PTRACE. The results were used to obtain values for the longitudinal and transverse acceptances and emittances for the RTM. The results indicate a stable acceleration with little longitudinal emittance growth for a synchronous phase of -20° and an injection phase of $+25^{\circ}$. The calculated acceptances of the RTM are 100π keV-deg longitudinally and 2π mm-mrad transversely.

EXPERIMENTAL EQUIPMENT

A full discussion of the planned physics program and the experimental equipment cannot be presented here. Interested readers are referred to ref. (2). The planned facility showing the RTM and experimental areas in the beam hall and Tandem room is shown in Fig. X. Major pieces of equipment planned for are tagged photon monochromator and a spectrometer.

TABLE I: RTM PARAMETERS

GENERAL	
Output current:	100μA
Longitudinal acceptance:	100π keV-deg
Longitudinal emittance:	105π keV-deg
Transverse acceptance:	2π mm-mrad
Transverse emittance:	0.2π mm-mrad
Input energy:	4.37 MeV
Output energy:	47.5 MeV
Number of orbits:	27
Magnet separation:	3.17 m
MAGNET	
Field intensity:	0.272 T
Main field excitation:	2 x 8645 A-T
Contrafield excitation:	2 x 1450 A-T
Radius, inner orbit:	0.060 m
Radius, outer orbit:	0.590 m
Magnet weight:	9.4 tonnes
RF SYSTEM	
Klystron:	Thomson-CSF 2075
Field gradient:	0.95 MV/m
Dissipated power:	23.8 kW
Beam power:	4.3 kW
Energy gain/turn:	1.58 MeV
Synchronous phase:	-20°
Injection phase:	$+25^{\circ}$

Tagged Photon Monochromator: Monochromatic photons can be produced in conjunction with a CW microtron by tagging. This is a method of identifying photons of known energy, in a continuous bremsstrahlung spectrum, by measuring the energy loss of the associated electrons coming from a radiator target, by means of a magnetic spectrometer. One of the best systems currently operating is that built by J.W. knowles of CRNL and T. Drake of the Univ. of Toronto (16). At present, it is installed at the MUSL facility. The monochromator has a momentum bite of 20% with an energy resolution better than 14 keV, when detecting 2-3.5 MeV electrons at a counting rate of 10^4 cps per wire. With improved wire counters and by detecting lower energy electrons these specifications can be improved to 10^6 cps per wire with a resolution of 3-5 keV. The installation of baffles restricting the angular range of the detected electrons will enhance the production of polarized photons. It is planned to install this monochromator at the Montreal facility in area 5 (see Fig. X) as soon as an electron beam is available, thus allowing a physics program to be immediately initiated.

Electron Spectrometer: A magnetic spectrometer with good resolution, large solid angle and the capability of being operated at 180° scattering angles for the study of magnetic transitions is also planned as a major piece of experimental equipment, to be located in area 2 (see Fig. X). We have not as yet decided upon a spectrometer design. At 50 MeV electron energy, multiple scattering in the vacuum windows will limit the precision of any software corrections, thus the required resolution should be achieved by optical design. The spectrometer should have medium resolution over a large momentum bite and solid angle, for coincidence experiments, and have the capability of higher resolution over a limited momentum range and reduced solid angle for detailed single arm experiments. The two designs presently being considered are the "Clam Shell", or inclined pole spectrometer (17), and the MEPS spectrometer design (18).

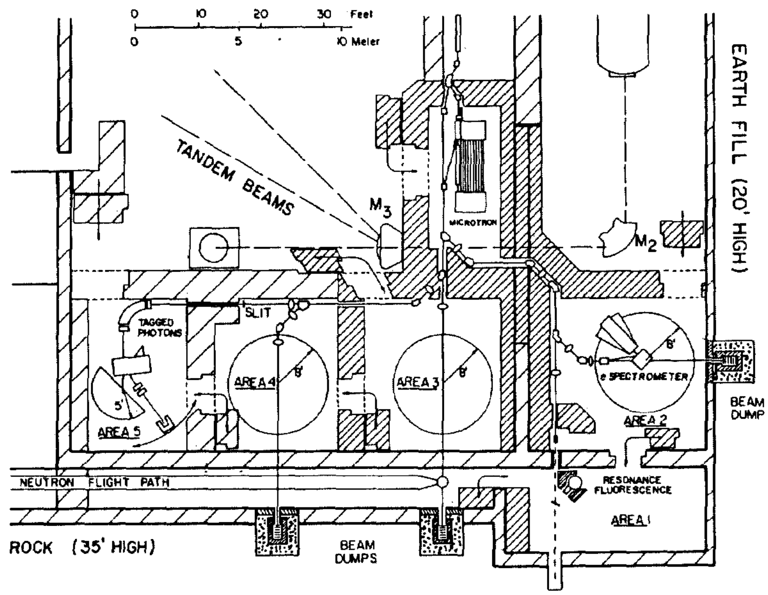

Fig. X:

Layout of the proposed facility in the existing beam hall and Tandem room in the present nuclear physics laboratory.

TABLE II: ACCELERATOR COST ESTIMATES

Electron gun:	100K$
Chopper-buncher:	54K$
LINAC structures:	660K$
Klystrons, power supplies:	625K$
RTM magnets, power supplies:	200K$
Computer controls:	200K$
RF lab requirements:	300K$
Beamline, vacuum system:	150K$
Beam control:	75K$
Radiation protection:	175K$
Machine shop facilities:	60K$
Building modifications:	400K$
Miscellaneous:	100K$
Manpower:	1671K$
Contigency:	465K$
TOTAL COST (Can.$):	5235K$

REFERENCES

(1) G.K. Bavaria, P. Depommier et al., Proposal for the Construction of a 1 GeV 100% Duty Cycle Electron Accelerator, unpublished, Nov. 1981.
(2) G.K. Bavaria, P. Depommier et al., Proposal for a 50 MeV Electron Facility, unpublished, July 1982.
(3) H. Herminghaus et al., NIM 138 (1976) 1.
(4) S. Penner and L.M. Young, NBS-LASL Microtron Design, June 1980, unpublished.
(5) K.R. Crandall, unpublished.
(6) J. McKeown, AECL-6406 (1979).
(7) K.H. Halbach and R.F. Holsinger, Part. Accel. 7 (1976) 213.
(8) A.A. Kolomensky, Thesis, Lebedev Institute, 1950.
(9) P.H. Debenham, Part. Accel. Conf., Wash., D.C. (1981) 2885.
(10) J.S. Colonias, UCRL-18439 (1968).
(11) R.F. Holsinger, NEN Report, 1978.
(12) V. Czok et al., NIM 140 (1977) 39.
(13) K.H. Kaiser, unpublished.
(14) J.S. Allen et al., Part. Accel., 1 (1970) 239.
(15) H. Babic and M. Sedlacek, NIM 56 (1967) 170.
(16) J.W. Knowles et al., NIM 193 (1982) 463.
(17) R.L. Boudrie, Workshop on High Resolution Large Acceptance Spectrometers, Argonne, Sept. 1981.
(18) I. Blomqvist, Symposium on Coincidence Spectrometers, Mainz, 1981.